The decline in arctic sea-ice thickness: Separating the spatial, annual, and interannual variability in a quarter century of submarine data

D. A. Rothrock,[1] D. B. Percival,[1] and M. Wensnahan[1]

[1] Naval submarines have collected operational data of sea-ice draft (93% of thickness) in the Arctic Ocean since 1958. Data from 34 U.S. cruises are publicly archived. They span the years 1975 to 2000, are equally distributed in spring and autumn, and cover roughly half the Arctic Ocean. The data set is strong: we use 2203 values of mean draft, each value averaged over a nominal length of 50 km. These values range from 0 to 6 m with a standard deviation of 0.99 m. Multiple regression is used to separate the interannual change, the annual cycle, and the spatial field. The solution gives a climatology for ice draft as a function of space and time. The residuals of the regression have a standard deviation of 0.46 m, slightly more than the observational error standard deviation of 0.38 m. The overall mean of the solution is 2.97 m. Annual mean ice draft declined from a peak of 3.42 m in 1980 to a minimum of 2.29 m in 2000, a decrease of 1.13 m (1.25 m in thickness). The steepest rate of decrease is −0.08 meters per year (m/a) in 1990. The rate slows to −0.007 m/a at the end of the record. The annual cycle has a maximum on 30 April and a peak-to-trough amplitude of 1.06 m (1.12 m in thickness). The spatial contour map of the temporal mean draft varies from a minimum draft of 2.2 m near Alaska to a maximum just over 4 m at the edge of the data release area 200 miles north of Ellesmere Island.

1. Introduction

[2] For several decades operational data from submarines have formed the primary basis of our observational knowledge of arctic sea-ice thickness. At first scientists used these data to characterize ice topography (pressure ridge statistics and the ice thickness distribution) and to characterize variability. By the 1980s enough data had accumulated to allow the spatial field of draft to be estimated, but it was clear that the contour maps had small-scale structure and seasonal differences affected by undersampling in both space and time [*Bourke and Garrett*, 1987; *Bourke and McLaren*, 1992]. Investigators began to use submarine data in about 1989 to address the question of interannual change. Because the timing and tracks of submarine cruises were designed to meet military objectives and not to provide optimal sampling of the spatial and temporal variability of sea ice, formulating analyses of the sparse and irregular data, either to map the field or to find a trend, has been problematic. There has been controversy about whether the data set is sufficiently strong to distinguish any signal of long-term change from "natural variability" [*McLaren et al.*, 1990; *Wadhams*, 1990]. Some studies have ignored the time

of year altogether. Some have segregated the data into summer or winter seasons, ignoring the facts that summer and winter data are related via the annual cycle and that the data are spread over seven months of the year. Some have focused on certain data-rich regions such as the North Pole or the strip from the pole to the Beaufort Sea roughly between 140° and 150°W. Some have compared data from two different clusters of years. Investigations focused on interannual change include *McLaren et al.* [1992], *Shy and Walsh* [1996], *Rothrock et al.* [1999], *Tucker et al.* [2001], *Winsor* [2001], and *Wadhams and Davis* [2000]. Table 1 summarizes some of the examinations of submarine ice draft data for signs of interannual change. Unanswered questions from these studies include, "Is the interannual signal truly discernible above the noise of 'natural variability'?" and, if so, "Is the interannual change one of continual decline or is the signal more complicated?".

[3] Over the decades, more and more data have become publicly available. Data on sea-ice draft from 34 U.S. Navy submarine cruises and two British cruises within the Arctic Ocean are now available at the *National Snow and Ice Data Center* [NSIDC, 2006]. The archived data consist of draft profiles at nominally one-meter spacing; there are on the order of 10^8 data points (100,000 km of profiles), along with summary statistics including the mean draft over roughly 50-km sections. The purpose of this paper is to analyze these mean draft data and determine what they reveal about sea-ice variability. We purposely avoid any use

[1]Applied Physics Laboratory, University of Washington, Seattle, Washington, USA.

Table 1. Investigations of Interannual Change Using Submarine Ice Draft Data

Reference	# of Cruises	Years Studied
NORTH POLE		
McLaren et al. [1992]	6	1977–1990
McLaren et al. [1994]	12	1958–1992
Shy and Walsh [1996]	12	1977–1992
FRAM STRAIT & LINCOLN SEA		
Wadhams [1990]	2	1976 cf. 1987
Wadhams and Davis [2000]	2	1976 cf. 1996
BEAUFORT SEA TO NORTH POLE		
McLaren [1989]	2	1958 cf. 1970
Tucker et al. [2001]	9	1976–1994
Winsor [2001]	6	1991–1997
SUBMARINE DATA RELEASE AREA (DRA)		
Rothrock et al. [1999]	9	1958–76 cf. 1993–97
Present	34	1975–2000

here of other sea-ice information, in particular, from sea-ice models. This analysis rests purely on the submarine data and has two strengths. First, the study makes use of data from 17 cruises recently placed at NSIDC [*Wensnahan et al.*, 2007; *Rothrock and Wensnahan*, 2007], providing a fairly continual record in both spring and autumn from 1975 to 2000 from the total of 34 U.S. cruises. Second, it capitalizes on the opportunity provided by this expanded data set to analyze all the U.S. submarine data as a single data set in order to separate the dependencies on space, on season, and on year. In taking this approach we begin to fulfill the vision of *McLaren et al.* [1990] who saw that "A direct approach would involve statistical analysis by season, region and ... for each year of all...under-ice thickness distribution data obtained by U.S. and British nuclear submarines since 1958. Only then might genuine trends be distinguished from natural variability." We would add that only then will a spatial climatological field and annual cycle be identified.

[4] We use multiple regression to determine how draft depends on the independent variables. The goal is to find a simple algebraic formula or regression model for draft as a function of space, season, and year, leaving residuals (discrepancies between the data and the regression model) that are small. We build the regression model by starting with terms of low order and adding terms of higher order, until the addition ceases to reduce the variance of the residuals significantly as determined by statistical tests. The regression model "explains" a portion of the variance in the data, leaving the remaining variance in the residuals as "unexplained" variance that can be considered as either error in the regression model or observational error or both. We adopt a regression model in which the spatial, annual, and interannual variations are separated and additive. Of course this form is somewhat subjective, guided by physical intuition, but, for instance, whether the spatial dependence should be linear or quadratic or cubic is determined by the data.

[5] In section 2, the data set is described and the variables defined. Section 3 presents the best fit multiple regression model and the coefficients of the fit: the seasonal cycle, the spatial field, and the interannual change. Section 4 gives the relationship between ice draft and the combined mass

of sea ice plus its snow cover and suggests that this observed ice-cover (ice-plus-snow) mass may be worth using to test models. Section 5 gives the relationship between draft and ice thickness. In section 6 these results are discussed in the context of previous results.

2. Data

[6] The data used here are from 34 cruises of U.S. Navy submarines from 1975 to 2000. Each cruise lasted roughly one month; the distribution of cruises by year and month is shown in Figure 1 (one dot per cruise). Originally classified secret, the data have been declassified and released for public use mostly within a data release area (DRA), an irregular polygon that lies within the Arctic Ocean and outside the "exclusive economic zones" of foreign countries (see Figure 2 and Table 2). Data in the archive have been acquired by two different recording systems: digital recording and paper chart. We believe that the data extracted by scanning U.S. paper charts and applying digital image processing techniques have been made equivalent (in the sense of being unbiased) to those acquired by digital
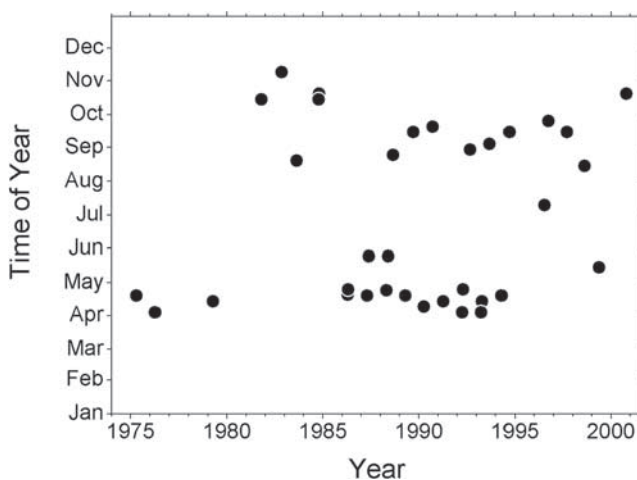
Figure 1. Thirty-four U.S. Navy submarines cruises from which sea ice draft data are analyzed.
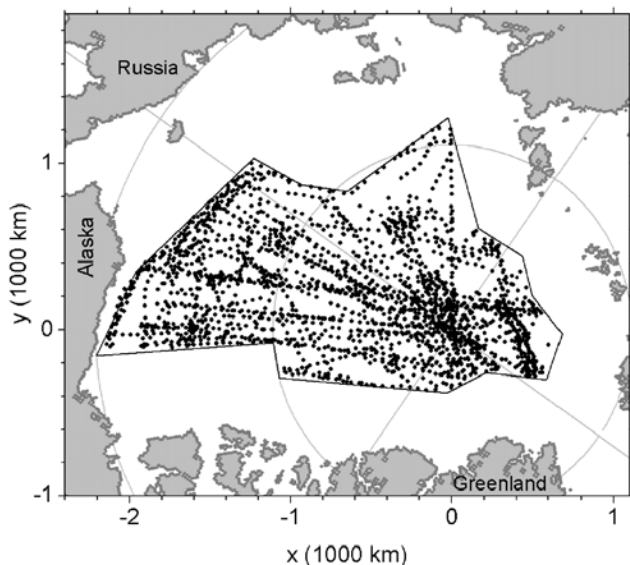
Figure 2. Data points from U.S. Navy cruises used in our analysis. The irregular polygon outlines the data release area (DRA): the "SCICEX Box," whose vertices are given in Table 2. The (x, y) coordinates are as defined in (1).

recording [*Wensnahan and Rothrock*, 2005]. We do not use here archived data from British cruises, because there are only two of them, much of their data is outside our study area, and their *manual* processing from paper charts may introduce a positive bias because of difficulty in resolving the troughs between ridges. For the same reason we also do not use here U.S. data that were *manually* digitized (the 1958–1976 data in *Rothrock et al.* [1999]).

[7] We use as our dependent variable the mean draft D in meters. The means are taken over nominal 50-km sections of a draft profile (with drafts given at one-meter spacings, so nominally 50,000 pings per 50-km mean). A length of 50 km has become a *de facto* standard for reporting submarine-derived ice draft statistics. As discussed at the end of section 3 and again in section 6, the observational error, which includes both sampling error [*Percival et al.*, 2008] and the sonar system measurement error [*Rothrock and Wensnahan*, 2007], has a standard deviation of 0.38 m. For archived sections less than 50 km long, data from multiple sections within 75 km of each other are combined in a cluster such that the *sample* length is between 25 and 55 km. Short sections that cannot be successfully clustered are discarded. These means include open water; they are not, as some investigators have considered, "ice-only" means that exclude from the average any ice thinner than some threshold, say, 30 cm.

[8] The first independent variable, which models interannual variation, is the decimal year t; for example, the first instant of 1988 is $t = 1988.000$, which happens to be very nearly at the midpoint of the data set's time span. The second variable is the decimal fraction of the year τ, which marks the seasons; it ranges from 0 to 1 over the course of a calendar year and is the fractional part of t. To fit the annual cycle in the regression model we use the two terms $\sin(2\pi\tau)$ and $\cos(2\pi\tau)$ to represent the fundamental frequency; for easier interpretation, these are later converted to a single

cosine function with a phase that gives the times of the annual maximum and minimum. The final two independent variables are spatial: x and y defined from latitude ϕ and longitude λ (in degrees) by

$$\rho = 2R^* \sin[(45° - 0.5\phi)\pi/180°]$$
$$x = \rho^* \cos[(\lambda - 35°)\pi/180°]/1000$$
$$y = \rho^* \sin[(\lambda - 35°)\pi/180°]/1000 \qquad (1)$$

where R = 6370 km is the radius of the Earth. The (x, y) coordinate system has its origin at the North Pole, and the positive x axis runs along 35°E, as illustrated in Figure 2. This transformation (Lambert azimuthal equivalent) maps the Earth's surface to a plane tangent at the North Pole; ρ is the straight-line distance from the Pole through the Earth to a point (x, y) on the surface. The mapping conserves area. The units of x and y are nominally 1000 km, but the transformation shrinks latitudinal distance and expands longitudinal distance as one moves away from the pole. At the pole, a degree of latitude is 111.17 km; at the extreme southern corner of the DRA ($\phi = 70°$), a degree of latitude is 109.48 km. The difference is negligible for our purposes.

[9] The dataset used here has 2203 records, each containing a mean draft with its time and position, and is available at the web site of the Polar Science Center, Applied Physics Laboratory, University of Washington under "Data Sets" [http://psc.apl.washington.edu/pscweb2002/data/datasets.html].

3. Result of the Multiple Regression

[10] The 2203 50-km mean draft values D range from 0 to 6.09 m. Their variance is 0.98 m^2. Multiple regression allows us to determine how much of this variance in D can be explained by the four variables: t, τ, x, and y.

[11] We first consider how well the individual variables can explain the data. A regression model using a linear term in just the year t explains only 28% of the variance. Using just the fundamental frequency of the season explains only 33% of the variance, and using just linear terms in x and y explains 26% of the variance. Clearly using all of these variables together in a multiple regression will do better, but how much better?

Table 2. Coordinates of Vertices Defining the Data Release Area (DRA), Known as the "SCICEX Box"[a]

Latitude, deg	Longitude (°E:+, °W:−)	x, 10^3 km	y, 10^3 km
87.00	−15.00	0.214 366	−0.255 471
86.58	−60.00	−0.033 104	−0.378 391
80.00	−130.00	−1.072 528	−0.287 386
80.00	−141.00	−1.107 658	−0.077 458
70.00	−141.00	−2.206 887	−0.154 326
72.00	−155.00	−1.962 697	0.346 071
75.50	175.00	−1.231 624	1.033 459
78.50	172.00	−0.933 494	0.870 501
80.50	163.00	−0.649 506	0.831 333
78.50	126.00	−0.022 275	1.276 201
84.33	110.00	0.163 001	0.608 326
84.42	80.00	0.438 730	0.438 730
85.17	57.00	0.498 047	0.201 224
83.83	33.00	0.684 883	−0.023 917
84.08	8.00	0.585 876	−0.298 519

[a]The conversion between (lat, long) and (x, y) is given in (1).
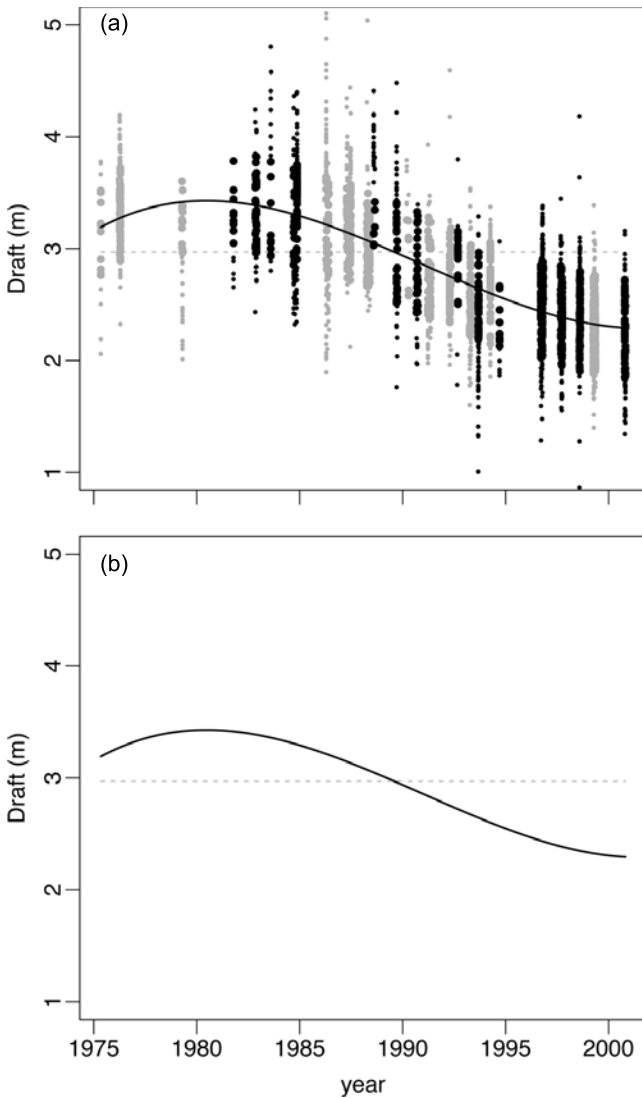
Figure 3. (a) The interannual change in the mean draft averaged over the DRA and the annual cycle, $\overline{D} + I'(t - 1988)$, in meters, along with the residuals [added to $\overline{D} + I'(t - 1988)$], black dots for summer/fall, grey dots for winter/spring. Each vertical line of dots comes from one cruise or, in a few cases, two nearly simultaneous cruises. Dots for residuals within one standard deviation of the curve are heavier. (b) The interannual change in the mean draft as in (a) but without the residuals.

[12] The simplest (linear) multiple regression equation treats the independent variables as separable

$$D(t, \tau, x, y) = C + I(t - 1988) + A(\tau) + S(x, y) + \varepsilon(t, \tau, x, y),$$
(2a)

where C is a constant, $I(t - 1988)$ describes the interannual change centered around 1988, $A(\tau)$ describes the annual cycle, and $S(x, y)$ is the spatial field. The inability of those four terms to completely reproduce the data D is measured by the errors (or residuals) ε, which we assume to obey a multivariate Gaussian distribution with a common mean of zero and variance of σ_ε^2. The ordinary least squares

(OLS) method determines C, I, A, and S in (2a) by minimizing the sum of squares of the residuals (estimated errors) and gives residuals that sum to zero. Under the Gaussian assumption, the OLS estimators of C and of the parameters specifying I, A, and S are unbiased and have a smaller variance than any other unbiased estimators if we make the additional assumption that the errors are independent of one another. However, *Percival et al.* [2008] show that there is weak long-range spatial correlation between 50-km means; the correlation function decreases slowly as a power law, $\sim d^{-0.46}$, for large separations d, rather than exponentially in d as, for example, for a common autoregressive process. This correlation must be taken into account to properly assess whether increasing the complexity of the functions I, A, and S in (2) is statistically warranted. Accordingly we assume independence of errors for different years and seasons, but a weak spatial correlation for errors within a given year and season that is dictated by long-range dependence. In the presence of such correlation, the OLS estimators are still unbiased, but the unbiased estimators with minimum variance are the generalized least squares (GLS) estimators [*Draper and Smith*, 1998]. We found that the standard deviations of the OLS-estimated parameters in (2a) are only 5% greater on average than those of the GLS method; that is, the spatial correlation has only a small effect on the multiple regression coefficients. In contrast to the GLS method, the OLS method allows exact partitioning of the variance of D, as done at the end of this section, so we report the OLS estimates in the following.

[13] Here we discuss the specific form of (2a) and its solution. The solution involves just the fundamental frequency in the annual cycle $A(\tau)$ and a cubic polynomial for $I(t-1988)$, while $S(x,y)$ has terms of 5th order, e.g., $x^3 y^2$. The solution for $S(x,y)$ retains all terms of a given order if any coefficients of that order are statistically significant at a 95% confidence level. The solution has 26 coefficients: the constant, three coefficients for I, two for A, and 20 for S. The data have a variance of 0.98 m². This solution to (2a) explains 79% of that variance leaving the unexplained variance (or the variance of the residuals), $\sigma_\varepsilon^2 = 0.21$ m².

[14] The value of C is 3.63 m, but this is not the mean, because neither I nor S is zero-mean. The mean of I over the 26 years 1975–2000 is $\overline{I} = -0.12$ m, and the mean of S over the DRA is $\overline{S} = -0.54$ m. The annual cycle averages to $\overline{A} = 0$. For simplicity, we define the zero-mean quantities
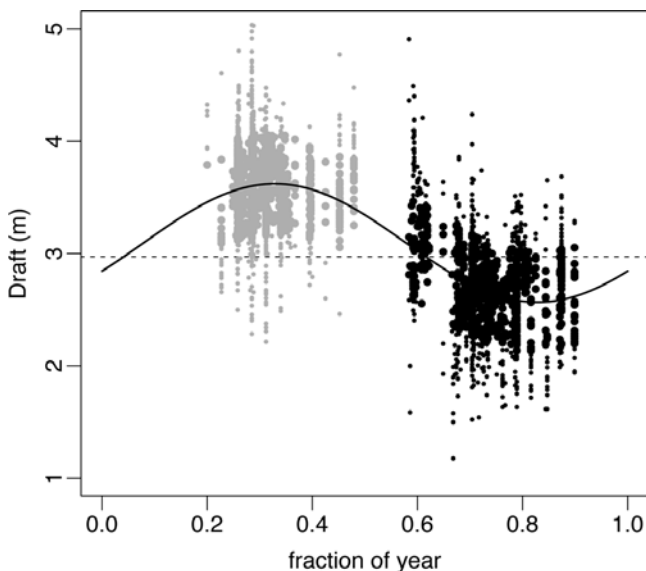
$$I' = I - \overline{I} \quad \text{and} \quad S' = S - \overline{S},$$

and a more convenient form of (2a)

$$D(t, \tau, x, y) = \overline{D} + I'(t - 1988) + A(\tau) + S'(x, y) + \varepsilon(t, \tau, x, y),$$
(2b)

in which each of the four right-hand terms has zero mean, and the mean draft from the regression model, averaged over 26 years, over a year, and over the DRA, is $\overline{D} = C + \overline{I} + \overline{A} + \overline{S} = 2.97$ m.

[15] The interannual change $I'(t - 1988)$ is depicted in Figure 3. It represents the interannual change in mean draft

Figure 4. The annual cycle of draft, $\overline{D} + A(\tau)$, in meters, averaged over the DRA and over the 26 years 1975–2000. The dots are the residuals [added to $\overline{D} + A(\tau)$], black for summer/fall, grey for winter/spring. Dots for residuals smaller than one standard deviation are plotted heavier.

averaged over the annual cycle and over the DRA. A linear dependence on t does not fit the data particularly well. The model draft rises for the first few years to a maximum of 3.42 m at year 1980.468 (21 June 1980), then falls by year 2000.816 (26 October 2000) to 2.29 m, a decrease of 1.13 m. Its most rapid decline occurs at the end of 1990 and is -0.08 m/a. By the end of the record the decline is much slower (-0.007 m/a). There is no sign in the model curve or in the data of a reversal or rebound by 2000. The multiple regression solution for $I(t - 1988)$ is

$$I(t - 1988) = I_1(t - 1988) + I_2(t - 1988)^2 + I_3(t - 1988)^3$$
$$I_1 = -0.0748$$
$$I_2 = -0.00219$$
$$I_3 = 0.000246$$
$$\overline{I} = -0.12 \tag{3}$$
$$I' = I - \overline{I}$$

The units of I_k are meters (year)$^{-k}$.

[16] The annual cycle $A(\tau)$ is shown in Figure 4. It represents the annual cycle averaged over the DRA and over the 26 years 1975–2000. The peak-to-trough amplitude is 1.06 m. The maximum occurs on 30 April ($\tau = 0.329$, day 120) and the minimum on 30 October ($\tau = 0.829$, day 303). The annual cycle is much larger than might be expected, given that this part of the ocean is mostly multiyear ice, and that a mature ice slab has a much smaller thermodynamic annual cycle of thickness [$\sim$0.43 m, *Maykut and Untersteiner*, 1971]. Sea-ice models show an annual cycle that is asymmetric, falling more steeply in the late spring and growing more slowly in autumn, but as seen from the residuals plotted around $A(\tau)$, the data are not dense enough throughout the year to resolve any harmonics and are sparse in just the period when the melt would be fastest (June and July, $\tau \sim 0.4$ to 0.6). The multiple regression solution for

$A(\tau)$ is

$$A(\tau) = A_{s0} \sin(2\pi\tau) + A_{c0} \cos(2\pi\tau) = A_0 \cos(2\pi[\tau - \tau_{\max}])$$
$$A_{s0} = 0.465$$
$$A_{c0} = -0.250$$
$$A_0 = 0.528$$
$$\overline{A} = 0$$
$$\tau_{\max} = 0.329 \tag{4}$$

The units of A_{s0}, A_{c0}, and A_0 are meters.

[17] The spatial field of draft is shown in Figure 5. This represents the spatial dependence of the mean draft, averaged over an annual cycle and the 26 years of the data record 1975–2000. The draft varies from 2.2 m near Alaska to just over 4 m near Ellesmere Island. The multiple regression solution for $S(x, y)$ is (using the notation $S_{ij}x^iy^j$ for each term)

$$S(x,y) = S_{10}x + S_{01}y$$
$$+ S_{20}x^2 + S_{11}xy + S_{02}y^2$$
$$+ S_{30}x^3 + S_{21}x^2y + S_{12}xy^2 + S_{03}y^3$$
$$+ S_{40}x^4 + S_{31}x^3y + S_{22}x^2y^2 + S_{13}xy^3 + S_{04}y^4$$
$$+ S_{50}x^5 + S_{41}x^4y + S_{32}x^3y^2 + S_{23}x^2y^3 + S_{14}xy^4 + S_{05}y^5$$

$$S_{10} = -0.7425, \ S_{01} = -0.4548$$
$$S_{20} = -0.5616, \ S_{11} = 0.4384, \ S_{02} = -0.9077$$
$$S_{30} = 1.1791, \ S_{21} = -0.3106, \ S_{12} = 1.5293, \ S_{03} = -1.6046$$
$$S_{40} = 0.8308, \ S_{31} = 0.5001, \ S_{22} = 6.8515, \ S_{13} = 0.3927,$$
$$S_{04} = 4.1612$$
$$S_{50} = 0.1389, \ S_{41} = 0.4178, \ S_{32} = 2.7062, \ S_{23} = -0.7921,$$
$$S_{14} = 0.5422, \ S_{05} = -2.0240$$
$$\overline{S} = -0.54$$
$$S' = S - \overline{S} \tag{5}$$

The units of S_{ij} are m/(10^3 km)$^{i+j}$. One can see that terms of higher order than linear are warranted by examining the two cases in Figure 6; in Figure 6a, S has been taken only to be linear in x and y and the spline (solid curve) fit through the
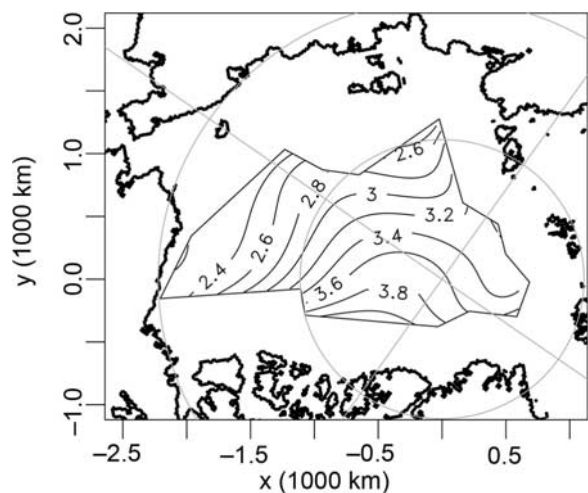
Figure 5. The spatial field of draft, $\overline{D} + S'(x, y)$, in meters, averaged over the 26 years 1975–2000 and over the annual cycle.
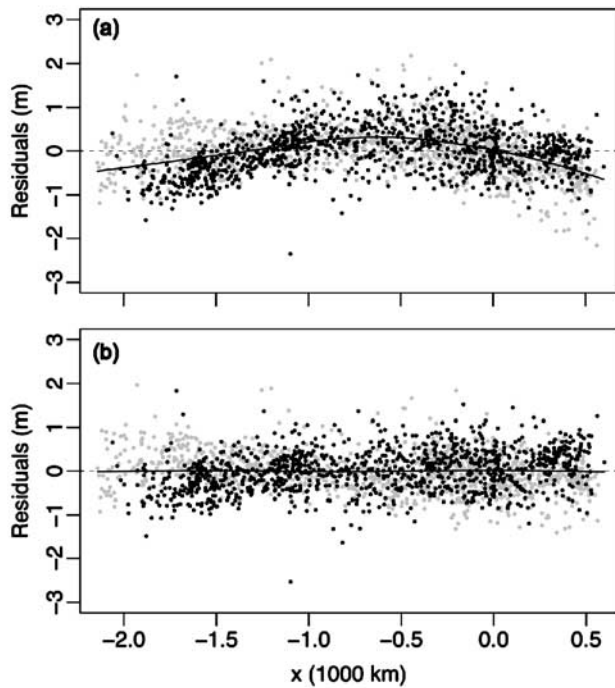
Figure 6. The residuals of the data (a) when $S(x, y)$ is a linear polynomial, and (b) for our solution when $S(x, y)$ is a 5th order polynomial, black for summer/fall, grey for winter/spring. The solid curves are spline fits to the residuals.

residuals shows strong higher order structure in x (but less in y, not shown). The final solution in (5) has 5th order terms that have incorporated that structure, leaving no apparent structure in the residuals (Figure 6b).

[18] By the nature of our choice of the form of (2a) and (2b), the shape of the field never changes. The field in Figure 5 also represents the 26-year mean field at the midpoints of the annual cycle, on 29 January ($\tau = 0.079$, day 29) and on 31 July ($\tau = 0.579$, day 212). Using (2), we can construct the field at other times or for other temporal integrals. To obtain the 26-year mean spatial field of draft for any time of year, we just need to add $A(\tau)$ to the map in Figure 5. For example, we add $A(0.329) = 0.53$ m for the spring maximum on 30 April or $A(0.830) = -0.53$ m for the autumn minimum on 30 October. Similarly, the mean annual field at any point between 1975 and 2000 can be computed by adding to the map in Figure 5 the quantity $I'(t - 1988)$. To average the field over a portion of the record from t_1 to t_2 (e.g., a period before the positive Arctic Oscillation anomaly in the early 1990s), we add to the map $\int_{t_1}^{t_2} I'(t - 1988)dt$.

[19] The 0.98 m^2 of variance in the data is partitioned as follows: 0.77 m^2 is explained by the regression model, (2), and 0.21 m^2 is unexplained and remains in the residuals. Figure 7 shows the probability density functions of the data and of the residuals with the range of both horizontal scales being 6 m. How should we view the 0.21 m^2 of unexplained variance? The error in the measurement system has a standard deviation of 0.25 m [*Rothrock and Wensnahan*, 2007], or a variance of 0.063 m^2. The error in sampling due to long-range dependence in the sea-ice cover has a

standard deviation of about 0.29 m for 50-km samples [*Percival et al.*, 2008], or a variance of 0.084 m^2. If we regard these two error sources as independent, we can add their variances (0.063 + 0.084) for an overall observational error variance of 0.147 m^2. So, the unexplained variance 0.21 m^2 is partitioned (as in Table 3) into an observational error variance of 0.147 m^2 and a remaining variance of 0.063 m^2 (standard deviation = 0.25 m) unable to be captured by (2). This value, a standard deviation of 0.25 m, represents the variability of the ice cover over and above both the observational error and what can be described by the regression model.

4. Ice and Snow Mass

[20] One useful property of ice draft is that it directly gives the combined ice and snow mass, the only assumption being the water density, which is extremely well known. By Archimedes' Principle, the mass of sea ice with its snow cover equals the mass of water displaced. With the water
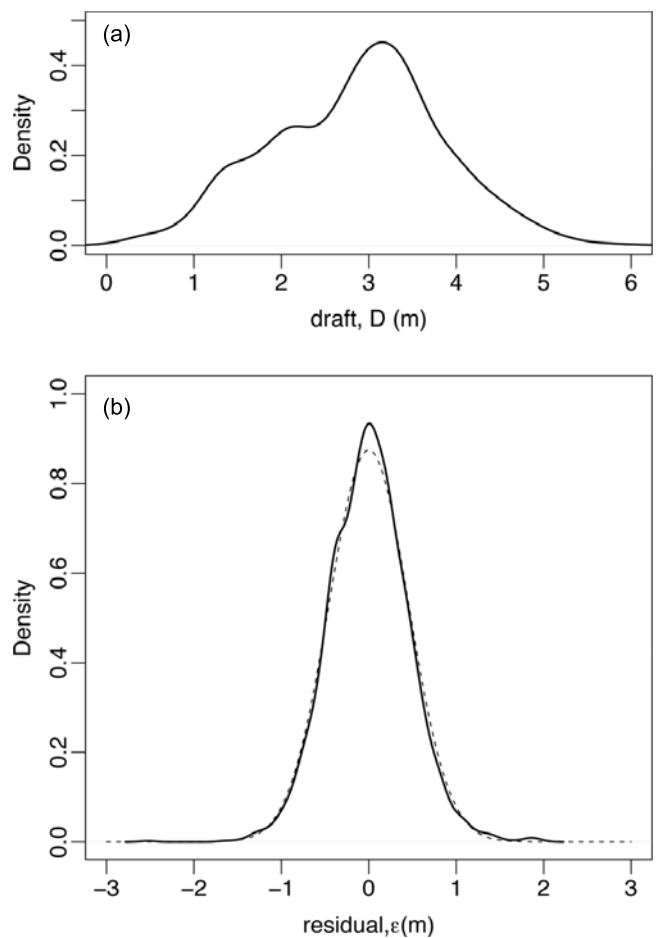
Figure 7. (a) The probability density function of observations of 50-km-mean ice drafts, with a standard deviation of 0.99 m. (b) The probability density function of residuals ε from the OLS fit to (2), with a standard deviation of 0.46 m, along with a Gaussian distribution (dashed) with the same standard deviation for comparison. The functions were generated using a kernel density estimator with bandwidths of 0.1907 and 0.8756.

Table 3. Variances and Standard Deviations in Draft

	Variance, m^2	Standard Deviation, m
Observed 50-km drafts	0.98	0.99
Residuals from OLS model (2)	0.21	0.46
Observational error	0.147	0.38
OLS model residuals variance less observational error variance	0.063	0.25

density $\rho_w = 1{,}027$ kg/m^3 and draft D in meters, the ice and snow cover mass is $\rho_w D$ in kg/m^2.

[21] Ice-plus-snow mass has not been given wide attention, either as a fundamental observation or as a model variable to be tested against data. Rather the tendency has been to think of ice thickness and snow cover separately. There could be merit in testing modeled ice-cover mass, since the observation is available so directly, without complicating assumptions.

5. Converting Draft to Thickness

[22] The conversion of draft D to thickness T is affected by the snow load resting on the ice. We account only for the seasonal variation in the snow load. Equating the weight of the ice freeboard and snow to the buoyancy of the submerged ice, we have the hydrostatic equation

$$\rho_i F + \rho_s SN = (\rho_w - \rho_i)D, \qquad (6)$$

where F is the height of the freeboard, and we take ice density $\rho_i = 928$ kg/m^3 and water density $\rho_w = 1{,}027$ kg/m^3. To obtain seasonally changing values of snow density $\rho_s(\tau)$ and snow thickness $SN(\tau)$, we use the mean monthly data over multiyear ice from the snow climatology of *Warren et al.* [1999, their Figures 11 and 13]. Eliminating F from (6) using $F + D = T$, we obtain

$$T = \frac{\rho_w}{\rho_i}D - \frac{\rho_s}{\rho_i}SN = 1.107D - f(\tau), \qquad (7)$$

where $f(\tau) = \frac{\rho_s(\tau)}{\rho_i}SN(\tau)$ is the snow ice equivalent (thickness) that peaks at 0.12 m in May and rapidly decreases to zero by August (see Table 4). The annual mean of f is $\bar{f} = 0.076$ m. Equation (7) says that the ice thickness would be 1.107 times the draft, except that some of it (f) is snow, not ice. If the ice is just at the margin of being submerged by the snow load, the ice freeboard vanishes, and (6) with $F = 0$ states that the ice buoyancy just balances the snow load, or

$$D_{sub} = \frac{\rho_s SN}{(\rho_w - \rho_i)}, \qquad (8)$$

whose value for each month is shown in the last column of Table 4. In our solution to (2), the ice never becomes thin enough to satisfy (8) and to be submerged.

[23] Setting aside the error term ε, the best fit multiple regression equation (2) can be converted to an equation for thickness using (7)

$$T = 1.107\left[\bar{D} + I'(t - 1988) + S'(x,y) + A(\tau)\right] - f(\tau). \qquad (9)$$

To illustrate a few conversions, the mean thickness from the regression model (9), averaged over 26 years, over an annual

cycle, and over the DRA, is $\bar{T} = 1.107[\bar{D}] - \bar{f} = 3.21$ m. The interannual change in ice thickness is shown in Figure 8, along with the annual cycle superimposed. Whereas annual- and area-mean draft declined by 1.13 m from its peak in 1980 to its low point in 2000, the thickness declined by 1.25 m. The annual cycle of thickness is only slightly affected by the changing snow load: the dates of the seasonal extremes in thickness differ negligibly (a day) from those for draft, and the peak-to-trough amplitude of thickness is 1.12 m ($\Delta T = 1.107\Delta D - \Delta f$, where Δ is the change between 30 April and 30 October). The contours of the spatial field in Figure 5 are values of draft. To read them as contours of thickness, multiply draft by 1.107 and then subtract 0.08; so the greatest printed contour of 4.00-m draft near Ellesmere Island becomes the 4.35-m contour of thickness, and the lowest contour of 2.20-m draft in the Beaufort Sea becomes the 2.36-m contour of thickness.

[24] The average ratio of draft to thickness is $\bar{D}/\bar{T} = 2.97/3.21 = 0.93$.

6. Discussion and Summary

[25] We analyzed the publicly archived data from U.S. submarines, separating out the interannual change, the annual cycle, and the climatological spatial field. The data support regression models with polynomials of 5th order. A preliminary (unpublished) investigation using only eleven cruises and ten years of data indicated that only the linear coefficients were significant. With 26 years of data, we expected to find significant 2nd order terms, but in fact the data support 3rd order temporal and 5th order spatial terms that show interesting and interpretable interannual and spatial structure. Of the 0.98 m^2 of variance in the data, the multiple regression model explains all but 0.21 m^2 (21%) with a standard deviation = 0.46 m. We regard the multiple regression (2) as giving the ice draft at any point in our spatial and temporal domain to within a standard deviation of 0.46 m.

[26] A reasonable error budget (Table 3) is that the observational error (the combined measurement and sampling errors, as discussed at the end of section 3) has a variance of 0.147 m^2 and a standard deviation of 0.38 m, and that the signal in the data explained neither by the regression model nor the observational error has a variance of 0.063 m^2 and a standard deviation of 0.25 m, which is the

Table 4. Monthly Mean Values of Snow Density ρ_s, and Snow Depth SN [from *Warren et al.* [1999], Figures 11 and 13], Along With the Correction Term $f(\tau)$ in (7 and 9), and (in Column 5) the Draft of Ice (8) That Could be Submerged With These Snow Loads[a]

Month	ρ_s, kg m^{-3}	SN, m	$f(\tau)$, m	$D_{sub}(\tau)$, m
January	308	0.263	0.087	0.815
February	318	0.286	0.098	0.918
March	327	0.313	0.110	1.031
April	328	0.333	0.118	1.106
May	329	0.343	0.122	1.144
June	348	0.300	0.113	1.059
July	383	0.062	0.026	0.244
August	219	0.018	0.004	0.037
September	246	0.096	0.025	0.234
October	271	0.185	0.054	0.506
November	291	0.223	0.070	0.656
December	301	0.250	0.081	0.759

[a]The mean of f over 12 months, $\bar{f}$, is 0.076 m.
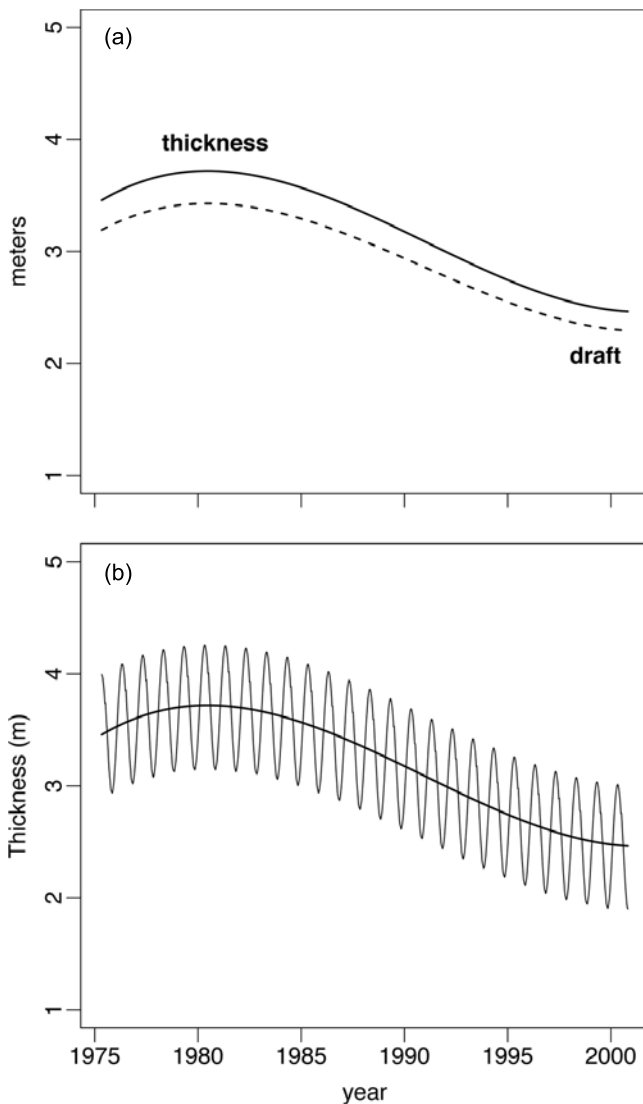
Figure 8. (a) The interannual change in areally and annually averaged ice thickness, $1.107[\overline{D} + I'(t - 1988)] - \overline{f}$. The dashed line is the draft in Figure 3. (b) The same thickness curve showing the annual cycle (dotted) superimposed, $1.107[\overline{D} + I'(t - 1988) + A(\tau)] - f(\tau)$.

"natural variability" not captured by the regression model. Of course the measurement errors may be less than estimated by *Rothrock and Wensnahan* [2007], and the "natural variability" may be a greater portion of the unexplained variance of the multiple regression model.

[27] The multiple regression solution sheds light on the question of whether digitized data from (analog) paper charts are comparable to digitally recorded (DIPS) data. The residuals from each type of data are statistically equivalent: the residuals from scanned paper charts have a mean of -0.05 m and a standard deviation of 0.47 m, and the residuals of the DIPS data have a mean of +0.03 m and a standard deviation of 0.45 m. This seems a good match to the finding [*Wensnahan and Rothrock*, 2005] that the two data types should agree to ±6 cm.

[28] There is also a positive bias in submarine data (caused primarily by the finite sonar beamwidth), which is estimated to be 0.29 m [*Rothrock and Wensnahan*, 2007].

The data should be reduced by 0.29 m when compared with any non-U.S.-submarine observation or with ice model output. This correction can be applied to our multiple regression solution by subtracting 0.29 from $\overline{D}$.

[29] The unexplained variance of 0.21 m^2 (standard deviation = 0.46 m) seems to be a very strong upper bound on the observational error in (25- to 55-km means of) the U.S. submarine ice draft data. It seems quite unlikely that the random observational error could be larger than this value. If it were, the data could not be represented by the smooth functions in (2) with an unexplained variance as low as 0.21 m^2.

[30] From the multiple regression solution we find that the mean ice draft over our temporal and spatial domain is 2.97 m (3.21 m for thickness). The interannual response (Figures 3 and 8) shows a high rate of decline centered around 1990, preceded by a maximum in 1980 and followed by a minimum in 2000 at the end of the record. The decline from the maximum to the minimum is 1.13 m in draft (1.25 m in thickness). If we correct for the bias estimated by *Rothrock and Wensnahan* [2007] by subtracting 0.29 m from all drafts, this change represents a decline of 36% from the maximum. It is less than the 43% decline reported by *Rothrock et al.* [1999]. That analysis compared data from an earlier period (1958–1976) with data in the 1990s, and, in addition, the earlier data had been *manually* digitized from paper charts and are likely of lower quality than the data used here, which are from *digitally* processed paper charts and digitally recorded data. The present analysis is based on a data set that is much more voluminous and of higher quality but spans a shorter period. The timing of the steepest decline agrees with the findings of *Tucker et al.* [2001], who also noted that the decline in draft was 1.5 m in the Canada Basin and insignificant at the North Pole. None of the older estimates of arctic ice thickness from Nansen's *Fram* expedition (1893–6), from Koerner's British Trans-Arctic Expedition (1968–9), or from the earliest submarine cruises (from 1958) is thinner than the 3 m we find here, and several are closer to 4 m [see *McLaren et al.*, 1990]. Whether this change is part of a cyclical or random variation or a stage in a continual, intermittent decline, it is a very large fractional change in mean ice draft! Through 2000 we see no sign that ice thickness is rebounding in this large area of the Arctic Ocean. What has happened since 2000 can only be answered by more recent data.

[31] The annual cycle $A(\tau)$ is large, 1.06 m peak-to-trough in draft (1.12 m in thickness), over twice that of a thermodynamically mature slab of ice. We do not know of previous observational estimates of the large-scale annual cycle amplitude. There are several possible reasons for an annual cycle of mean draft larger than that of a slab of 3-m thick ice. First, thin ice has a larger cycle than a "mature" floe, forming most prolifically in autumn, growing very rapidly in early winter, and melting more in summer. Second, the annual cycle in ridged ice is likely larger than a 3-m-thick floe: ridges are formed rapidly in early winter from an abundance of thin ice, and they have been observed to melt 60% more than undeformed ice [*Perovich et al.*, 2003, their Figure 7b]. So, both the thin and the thick ends of the ice thickness distribution likely have a larger annual cycle than that of mature, level ice. In numerical sea-ice models that include a full thickness distribution, the range of the annual cycle is over 1 m: *Flato and Hibler* [1995] show a volume amplitude of ~1×10^4 km^3, which trans-

lates to ~1.3 m in draft (taking an Arctic Ocean area of ~7 × 10⁶ km²), and *Rothrock et al.* [1999, Figure 2] also show a modeled annual cycle of draft of about 1.3 m. Third, the annual cycle (30 April – 30 October) of draft is enhanced by the annual cycle of the snow load (section 5) by about 0.06 m. The phase of the annual cycle is in line with other observations and with sea-ice models.

[32] Several previous investigators have produced contour maps of draft over sizable portions of the Arctic Ocean. The spatial field in Figure 5 has structure that resembles some of these. The LeSchack field [*Bourke and McLaren*, 1992, Figure 1] using data from the 1960s and 1970s shows a long-term mean field for the Pacific side of the North Pole. Our field agrees with that estimate at the Pole, but differs by up to 1 m elsewhere. (For example, compared with our field the LeSchack field is +1 m at the location of maximum draft in the DRA off Ellesmere Island, +0.5 m at the southern tip of the DRA at Alaska, and -0.6 m at the tip of the DRA pointed at the Laptev Sea.) The fields given by *Bourke and Garrett* [1987] (using 17 submarine cruises during 1960–1982 and other forms of data) are different from ours. Theirs is the "ice-only" mean draft; open water is excluded from their mean, although the threshold for exclusion is not given. The ice-only mean has the property that the annual cycle is inverted, although it is not clear why the inversion is so strong. In their Table 2, the minimum occurs in spring, the maximum in summer. The shapes of their summer and autumn fields resemble the shape in our Figure 5. The contour maps of *Bourke and McLaren* [1992] (using data from 12 submarine cruises during 1958–1987) show detail that seems to arise from attempting to contour around sparse data from different cruises, where temporal change has occurred. We find no suggestion in our data of the 4-m ice they show in the southern Beaufort Sea and Chukchi Sea, but ice model results during periods of strong anticyclonic circulation show that thick ice is advected into those seas and into the East Siberian Sea. Note that both the papers by Bourke report results from outside the DRA; this was accomplished by working with classified data to obtain the contour maps, which were then declassified. Those raw data (along-track draft profiles) are not publicly archived.

[33] How ubiquitous and widespread is the interannual change? By separating temporal from spatial variation, the present formulation (2) does not quantify regional variations of interannual change and the annual cycle; that study should be done with the data at hand. Without more data from outside the DRA, one cannot answer clearly the question of whether there is a "sloshing" mode such that ice at one time resident in the DRA moves out into Russian waters in eastern longitudes or into the western longitudes between the DRA and Canada, Ellesmere Island, and Greenland [*Holloway and Sou*, 2002; *Rothrock and Zhang*, 2005]. In this regard, our understanding of arctic sea-ice thickness would greatly benefit by an analysis of all Arctic Ocean draft data dating back to 1958 and extending outside the present DRA. As for the present and future, it would be a tragedy for arctic science if the U.S. Navy submarine fleet were unable to continue to collect and provide sea-ice draft data on future cruises.

References

Bourke, R. H., and R. P. Garrett (1987), Sea ice thickness distribution in the Arctic Ocean, *Cold Reg. Sci. Technol.*, 13(3), 259–280.

Bourke, R. H., and A. S. McLaren (1992), Contour mapping of arctic basin ice draft and roughness parameters, *J. Geophys. Res.*, 97(C11), 17,715–17,728.

Draper, N. R., and H. Smith (1998), *Applied Regression Analysis*, 3rd ed., 706 pp., Wiley-Interscience, New York.

Flato, G. M., and W. D. Hibler III (1995), Ridging and strength in modeling the thickness distribution of arctic sea ice, *J. Geophys. Res.*, 100(C9), 18,611–18,626.

Holloway, G., and T. Sou (2002), Has arctic sea ice rapidly thinned?, *J. Clim.*, 15(13), 1691–1701.

Maykut, G. A., and N. Untersteiner (1971), Some results from a time-dependent thermodynamic model of sea ice, *J. Geophys. Res.*, 76(6), 1550–1575.

McLaren, A. S. (1989), The under-ice thickness distribution of the Arctic Basin as recorded in 1958 and 1970, *J. Geophys. Res.*, 94(C4), 4971–4983.

McLaren, A. S., R. G. Barry, and R. H. Bourke (1990), Could arctic ice be thinning?, *Nature*, 345(6278), 762.

McLaren, A. S., J. E. Walsh, R. H. Bourke, R. L. Weaver, and W. Wittmann (1992), Variability in sea-ice thickness over the North Pole from 1977 to 1990, *Nature*, 358(6383), 224–226.

McLaren, A. S., R. H. Bourke, J. E. Walsh, and R. L. Weaver (1994), Variability in sea-ice thickness over the North Pole from 1958 to 1992, *Polar Oceans and Their Role in Shaping the Global Environment*, edited by O. Johannessen et al., Amer. Geophys. Union.

National Snow and Ice Data Center (2006), *Submarine upward looking sonar ice draft profile data and statistics*, Boulder, Colorado USA: National Snow and Ice Data Center/World Data Center for Glaciology. Digital media.

Percival, D. B., D. A. Rothrock, A. S. Thorndike, and T. Gneiting (2008), The variance of mean sea-ice thickness: Effect of long-range dependence, *J. Geophys. Res.*, 113, C01004, doi:10.1029/2007JC004391.

Perovich, D. K., T. C. Grenfell, J. A. Richter-Menge, B. Light, W. B. Tucker, and H. Eicken (2003), Thin and thinner: Sea ice mass balance measurements from SHEBA, *J. Geophys. Res.*, 108(C3), 8050, doi:10.1029/2001JC001079.

Rothrock, D. A., and M. Wensnahan (2007), The accuracy of sea-ice drafts measured from U.S. Navy submarines, *J. Atmos. Oceanic Technol.*, doi:10.1175/JTECH2097.1.

Rothrock, D. A., and J. Zhang (2005), Arctic Ocean sea ice volume: What explains its recent depletion?, *J. Geophys. Res.*, 110, C01002, doi:10.1029/2004JC002282.

Rothrock, D. A., Y. Yu, and G. A. Maykut (1999), Thinning of the Arctic sea-ice cover, *Geophys. Res. Lett.*, 26(23), 3469–3472.

Shy, T. L., and J. E. Walsh (1996), North Pole ice thickness and association with ice motion history 1977–1992, *Geophys. Res. Lett.*, 23(21), 2975–2978.

Tucker, W. B., J. W. Weatherly, D. T. Eppler, L. D. Farmer, and D. L. Bentley (2001), Evidence for rapid thinning of sea ice in the western Arctic Ocean at the end of the 1980s, *Geophys. Res. Lett.*, 28(14), 2851–2854.

Wadhams, P. (1990), Evidence for thinning of the arctic ice cover north of Greenland, *Nature*, 345(6278), 795–797.

Wadhams, P., and N. R. Davis (2000), Further evidence of ice thinning in the Arctic Ocean, *Geophys. Res. Lett.*, 27(24), 3973–3975.

Warren, S. G., I. G. Rigor, N. Untersteiner, V. F. Radionov, N. N. Bryazgin, Y. I. Aleksandrov, and R. Colony (1999), Snow depth on arctic sea ice, *J. Clim.*, 12(6), 1814–1829.

Wensnahan, M., and D. A. Rothrock (2005), Sea-ice draft from submarine-based sonar: Establishing a consistent record from analog and digitally recorded data, *Geophys. Res. Lett.*, 32(11), L11502, doi:10.1029/2005GL022507.

Wensnahan, M., D. A. Rothrock, and P. Hezel (2007), New arctic sea ice draft data from submarines, *EOS*, 88(5), 55–56.

Winsor, P. (2001), Arctic sea ice thickness remained constant during the 1990s, *Geophys. Res. Lett.*, 28(6), 1039–1041.

———————————

D. B. Percival, D. A. Rothrock, and M. Wensnahan, Applied Physics Laboratory, University of Washington, Box 355640, Seattle, WA 98195, USA. (rothrock@apl.washington.edu)